Competition between vitrification and crystallization of methanol at high pressure

Brugmans, M.J.P.; Vos, W.L.

Published in:
Journal of Chemical Physics

DOI:
10.1063/1.470526

Competition between vitrification and crystallization of methanol at high pressure

Marco J. P. Brugmans
FOM-Institute for Atomic and Molecular Physics, Kruislaan 407, 1098 SJ Amsterdam, The Netherlands

Willem L. Vos
Van der Waals–Zeeman Laboratorium, Universiteit van Amsterdam, Valckenierstraat 65-67, 1018 XE Amsterdam, The Netherlands

(Received 16 February 1995; accepted 10 May 1995)

We have studied methanol at high pressure up to 33 GPa at room temperature with x-ray diffraction, optical (polarization) microscopy, Raman spectroscopy, and detection of hydrostaticity. A competition between crystallization and vitrification is observed when methanol is superpressed beyond the freezing pressure of 3.5 GPa: between 5.0 and 10.5 GPa crystals can nucleate, but if this region is surpassed quickly enough (within a few seconds), methanol remains amorphous. For the first time the nucleation rate and the crystal growth velocity have been studied as a function of pressure. These kinetic properties can be described by classical nucleation theory in agreement with, respectively, Turnbull–Fisher and Wilson–Frenkel type behavior using one and the same activated hard-sphere diffusion coefficient. The experimental nucleation rate and the crystal growth velocity are both effectively reduced to zero above 10.5 GPa, because the diffusion is suppressed. At these pressures methanol is compressed into a glass. © *1995 American Institute of Physics.*

I. INTRODUCTION

Glasses are subject to intensive study because they are of considerable technological interest, whereas their physical description is still far from complete.[1,2] A promising description of glass forming liquids is by a potential energy hypersurface Φ in configuration space (see, e.g., Refs. 3–7). This potential energy landscape Φ is a function of the positions of all particles, and one point on Φ corresponds to a definite arrangement of all particles. In the liquid phase the system has so much kinetic energy that it probes all configuration space. In a solid phase the system is trapped in a minimum of Φ, which means that it samples only a limited part (a basin) of configuration space. The energetically most favorable absolute minima in Φ correspond to the crystalline phase of the solid. However, when the system is trapped in a basin of the potential energy landscape different from the absolute minima, the system is in a (nonequilibrium) glassy state. From this description it is readily inferred that the glassy phase can be reached when the solidification is rapid enough so that the system is trapped before it can relax to an absolute (crystalline) minimum. Thus competition between crystallization and vitrification is expected at certain solidification rates.

The usual method to form a glass is by rapid cooling of a liquid.[1] If the system is quenched into a relative minimum in Φ, relaxation to lower lying basins in Φ can take place. If the remaining kinetic energy is so low that the time it takes to traverse the energy barriers to the next potential well is longer than practical time scales (hours), the system is effectively trapped and is for all practical purposes a glass. A complementary way to vitrify a liquid is by applying pressure.[8–10] In this way no kinetic energy is withdrawn from the system, but the energy barriers that connect different regions in configuration space are increased in height, and their spacing is decreased due to compression. For pressures higher than the glass transition pressure, the system is trapped between barriers. If the system is in a potential well different from the wells corresponding the crystal states and relaxation to other potential wells is again slow compared to the experiment, the system has been compressed into a glass.

Because glass formation and relaxation phenomena in this nonequilibrium state are still insufficiently understood, it is of interest to compare pressure induced vitrification with predictions based on the more usual temperature quenching.[6] In addition, temperature quenching experiments are usually performed isobarically, hence in addition to the temperature also the density is changed (by up to 25% in methanol[11]). In contrast, in isothermal compression only the density is varied which might simplify the comparison with theory. We study pressure induced vitrification of methanol because methanol is a simple hydrogen-bonded glass forming system.[12,13]

Temperature quenched methanol glasses are usually obtained by vapor deposition onto a cold ($<$110 K) substrate,[11,14–16] as it is difficult to freeze a liquid sample fast enough to obtain the glassy state (although that method has been reported[17]). Slower freezing from the liquid state yields an orthorhombic[18] crystalline β phase at higher temperature (157 K$\leqslant T \leqslant$175 K). A crystalline α phase is formed at lower temperature,[14,15] that is probably monoclinic.[18] Applying pressure to methanol at room temperature leads, according to the general notion in the literature,[19] to formation of a glass around 8.6 GPa. This apprehension is based on the occurrence of pressure gradients at this pressure as determined by Piermarini *et al.*[20] Recently, however, it was suggested that at this pressure methanol solidifies into a crystalline state rather than becoming a glass, because the viscosity is found to be 8 orders of magnitude lower than the glass defining value.[21] From these viscosity measurements a glass transition pressure of 11 ± 0.7 GPa was anticipated. The equilibrium melting pressure at room temperature is around 3.5 GPa.[20,22]

From Raman spectroscopy it has been deduced that the pressure induced crystalline structure resembles that of the low temperature α phase.[22] It seems better established that crystallization of methanol can be suppressed by addition of ethanol: The well known hydrostatic pressure medium of a 4:1 mixture of methanol to ethanol (4:1-M:E) starts to develop pressure gradients near 10.4 GPa.[20] At 10.8 GPa, Eggert *et al.*[23] have observed a change of the slope of the refractive index as a function of pressure, reminiscent of the temperature dependent behavior at the glass transition.[24]

We study pressurized methanol by x-ray diffraction, Raman spectroscopy, optical (polarization) microscopy, and hydrostaticity measurements. We find that liquid methanol at room temperature is always superpressed up to about 5.0 GPa. From 5.0 GPa to about 10.5 GPa there is a transition region where crystallization can occur. The x-ray diffraction decisively shows the lack of long range order in samples above 10.5 GPa that have not crystallized and the occurrence of large pressure gradients reveal that it is solid. In addition from the absence of optical polarization coloring, and from the absence of splitting of the C–O stretch Raman band, we conclude that this phase is the pressure induced glassy state of methanol.

Density dependent studies of the crystallization mechanism and the kinetics involved have so far only been explored in colloidal systems.[25–27] Because the crystalline phase of pressurized methanol can easily be recognized with optical microscopy and the crystal growth rate is slow enough for direct observation, we have been able to perform a detailed study of the crystallization kinetics. This is the first study of crystallization kinetics as function of pressure, or density, in a molecular system under isothermal conditions. The pressure dependencies of both the nucleation rate and the crystal growth rate can be described by a competition between the chemical potential difference and diffusion, giving rise to the competition between crystallization and vitrification of methanol at high pressures.

II. EXPERIMENT

Methanol used in the experiments was obtained from Merck with a stated purity of 99.8+%. For one set of samples a dehydrated form was used, containing less than 0.005% water. The methanol was used without further purification but was handled in a nitrogen environment to prevent water contamination. The samples were compressed in Diacell, Mao-Bell, Merrill-Bassett, membrane, and Silvera–Wijngaarden diamond–anvil cells (DAC).[28] The methanol was injected into 0.12 to 0.25 mm holes in tungsten or steel gaskets between the diamonds.

Small ruby grains in the gasket hole allowed for *in situ* determination of the pressure by the usual ruby fluorescence technique,[29] with a precision of about 0.05 GPa. By measuring the pressure at several ruby grains within one sample, pressure gradients could be detected, which indicate deviation from hydrostatic equilibrium and thus demonstrate solidification of the sample.[30]

For the Raman measurements the sample was excited by light from an Ar^+ laser using the 488 or 514 nm lines. Spectra were recorded with a Dilor XY triple monochromator equipped with a liquid nitrogen cooled CCD detector.

Angle dispersive x-ray diffraction experiments were carried out on station 9.1 at SRS, Daresbury Laboratory, UK (see Ref. 31) using the Edinburgh image-plate setup as described in Ref. 32. A double-bounce Si(111) monochromator was used to select a wavelength of 0.4652 or 0.4447 Å and the beam was collimated by a 200 μm platinum pinhole (130 μm for the highest pressure samples). The sample was carefully aligned with the beam and diffraction patterns were collected on image plates at about 18 cm distance from the DAC. The storage-phosphor image plates were read and the data were subsequently transferred to a workstation. Dedicated software[33] was used to perform integration over the Debye–Scherrer rings. To obtain the 2θ diffraction angle calibration, diffraction patterns were collected for materials with known d spacings: either InSb powder at ambient pressure loaded in the DAC or the tungsten gasket, after slight displacement of the cell.

III. RESULTS AND DISCUSSION

A. Phase identification

Optical microscopy proved to be a clarifying tool to examine methanol at high pressure: Samples compressed up to about 5.0 GPa look perfectly clear and, as is revealed using two polarizers, show no depolarization, consistent with the observations of Yenice *et al.*[34] For pressures in the range between about 5.0 and 10.5 GPa, many of the samples obtain a facetlike morphology as is shown in Fig. 1(a). Upon reaching pressures in this range, the change is often instantaneous or takes place after a few seconds, but especially at the highest pressures the conversion to facets is sometimes delayed by up to several hours (e.g., more than 2 h for a sample at 9.7 GPa). Especially at the higher pressures we could follow the conversion visually: We observed needles start to grow in clear samples within a few seconds or minutes, leaving behind a facetlike morphology, see Fig. 1(b). Most of the time needles grow through the whole sample from a single center (usually located at the edge of the sample), sometimes there are a few centers and on one occasion many nucleation sites were observed. After conversion from a clear to a facetlike morphology, the pressure was found to be lowered a few tenths of a GPa typically. Pressure gradients (e.g., a difference of 0.6 GPa between two ruby grains in a sample at 9 GPa, see Table I) reveal that the faceted sample is solid. Upon releasing the pressure the facets persist up to the melting pressure that we determine to be at 3.5 GPa, in good agreement with the previously reported values.[20,22] Using polarizers, we nearly always see polarization colors in the faceted samples, that become stronger upon releasing the pressure until the melting pressure is reached. When all grains are melted the sample looks clear again without polarization colors.

When a clear sample is rapidly pressurized from below 5.0 GPa to above 10.5 GPa, typically within a few seconds, the sample remains clear and does not exhibit polarization coloring [Fig. 1(c)]. The occurrence of pressure gradients, see Table I, shows that these clear high-pressure samples are

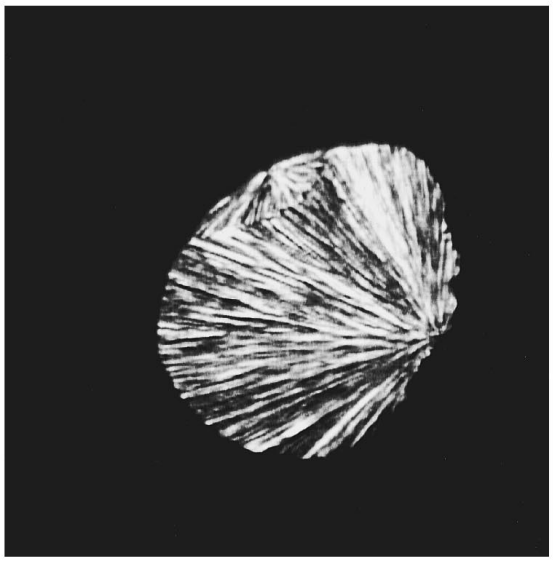
(a)

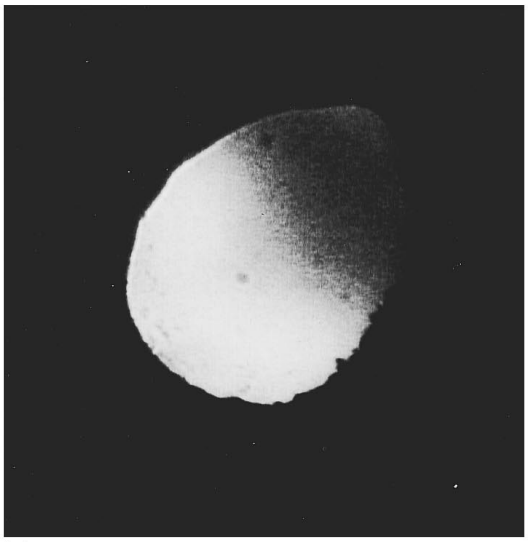
(c)

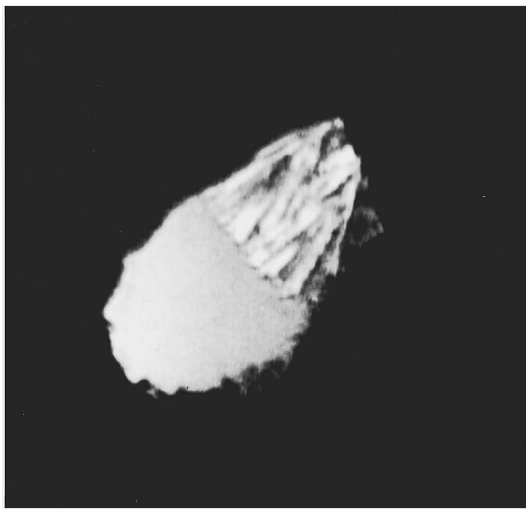
(b)

FIG. 1. Photographs of methanol as seen through a microscope with the sample between crossed polarizers for different pressures and different states. Above 5 GPa the sample morphology can become facetlike, as is shown for a sample at 8.2 GPa (a). Most of this morphology has grown from one center (right). A second center from which the conversion started somewhat later is also observed (upper left). The conversion process can be followed real time: in (b) needles are growing in a clear sample at 9.7 GPa. For this sample the total conversion from a clear sample to the morphology shown in (a) took about 20 min. Samples that are compressed fast enough above 10.5 GPa remain clear, which is illustrated in (c) for a sample at a pressure of 24 GPa. The depolarization is caused by stress in the diamonds of the DAC.

solid. When the pressure is subsequently reduced to below 10.5 GPa, the clear sample is often converted to a faceted morphology like the one that is shown in Fig. 1.

Raman spectra were taken up to about 24 GPa. The C–O stretch mode at 1031 cm^{-1} was found to be most indicative for the structural changes in the sample. Whereas the clear samples up to 5.0 GPa show a single C–O stretch Raman band, for the facet-morphologic samples the C–O stretch peak is clearly split. For clear samples above 12 GPa, a single broad C–O stretch band is observed that is decreased dramatically in intensity, but in the weak signal there is no indication for band splitting.

TABLE I. Largest pressure difference Δp between ruby grains at different pressures as observed for several samples.

Morphology	Phase	p (GPa)	Δp (GPa)
Clear	Liquid	4.5	0.06
		6.5	0.21
Faceted	Crystalline	7.7	0.54
		9.0	0.60
		17	1.78
Clear	Glassy	12.2	0.68
		13	2.60
		22	6.65
		24	6.40
		29	7.44

In Fig. 2 the x-ray diffraction patterns are shown for liquid methanol at 2.8 GPa, a facet-morphologic sample at 9.0 GPa, and a clear sample at 13.0 GPa. In contrast to the spectrum at 2.8 GPa, the scattered intensity from the facetedlike methanol exhibits pronounced peaks as function of 2θ, indicating long range order in the sample. For the clear sample at 13 GPa, however, no sharp diffraction peaks are observed. This spectrum is similar to the liquid at 2.8 GPa, with the main feature near $2\theta=8°$ shifted to larger diffraction angles due to compression. (The broad bump at $2\theta=20°$ is Compton scattering from the diamonds and from the sample.) In fact, in 15 x-ray diffraction patterns taken from 6 samples at different pressures we always observed sharply

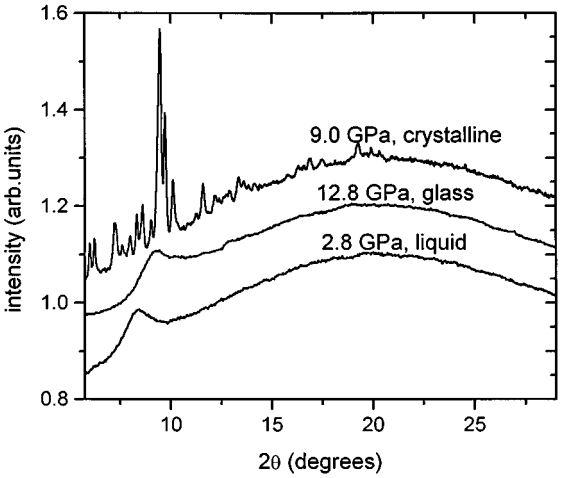

FIG. 2. X-ray diffracted intensity as a function of diffraction angle 2θ, for clear methanol samples at 2.8 and 12.8 GPa, and for a facetlike sample at 9.0 GPa. The spectra are the result of integration over Debye–Scherrer rings on the image plate. The curves have been scaled so that they coincide for large values of 2θ, and the 2 upper curves have been shifted 0.1 and 0.2 units, respectively. (The broad feature at $2\theta=20°$ is Compton scattering from both the cell and the sample.) Note the distinct difference between diffracted signals from crystalline and amorphous phases. The diffraction pattern of the glass resembles that of the liquid, with the features shifted to larger diffraction angles due to compression. The main diffraction peaks in the crystalline spectrum are at somewhat larger diffraction angles, corresponding to smaller distances, suggesting that the density of crystalline methanol at 9.0 GPa is larger than that of methanol glass at 12.8 GPa.

peaked diffraction patterns for the facet-morphologic samples and broad features for the clear samples. At the higher pressures (above 20 GPa) we find a small change in the shape of the first broad diffraction peak for the clear samples, indicating a structural change at these high pressures.[35] For the clear samples the intensity is homogeneously distributed over the Debye–Scherrer rings. The x-ray diffraction patterns of the facetlike samples consist of sharp rings, over which the intensity varies strongly indicating a strong preferred orientation. This all suggests that the facetlike samples, which display strong diffraction peaks, are crystalline and that the clear samples are amorphous. Note that this is consistent with the higher density for the facetlike samples at 9.0 GPa compared to the clear sample at 12.8 GPa, as inferred from the shift of the main diffracted intensity to higher diffraction angles.

From the splitting of the crystalline peaks we estimate that the peaks would be washed out for structures composed of less than ten unit cells.[36] Hence, the smooth diffraction patterns are associated with amorphous structures. In addition, when the pressure on clear high pressure samples is reduced a growth of facets from one or several points (nucleation centers) can be observed between 5.0 and 10.5 GPa. It is very unlikely that a polycrystalline phase with very small crystallites ($<$10 unit cells) regrows to larger crystals, starting from only one or a few centers. Also for the 4:1-M:E mixture in which the ethanol restrains crystallization, we obtained for pressures up to 12 GPa smooth diffraction patterns resembling the smooth curves in Fig. 2. Thus from the smooth diffraction patterns, from the presence of pressure gradients, from the absence of polarization coloring, and from the absence of splitting of the C–O stretch Raman band, we identify the clear samples above 10.5 GPa as methanol glass.

The notion in literature that methanol can be vitrified at high pressures is based on two studies. The first is that of Piermarini *et al.*,[20] in which a sudden increase of the linewidth of R_1 ruby fluorescence as a function of pressure was observed at 8.6 GPa, signaling the occurrence of pressure gradients. This was interpreted as the glass transition. The second proposition for pressure induced methanol glass was done in a Raman study of Mammone *et al.*[22] From broad and nonsplit Raman bands up to 9.2 GPa it was inferred that methanol is amorphous, in contrast to the sharp split peaks of crystalline samples. Raman spectra for these crystalline samples showed narrower peaks, and the C–H and C–O vibrations were split and displayed discontinuities as a function of pressure. In a recent study however, Cook *et al.*[21] extrapolated pressure dependent viscosity data to a glass transition pressure (defined as the point where the viscosity is 10^{13} P[6]) of 11.0 ± 0.7 GPa. Because they find viscosities as small as 10^5 P at a pressure of 8.35 GPa, they conclude that the pressure gradients observed by Piermarini *et al.* at 8.6 GPa[20] must be the result of crystallization, which they observed as a sluggish process at 8.5 GPa.

The observation of birefringence for the faceted sample supports the notion that it is crystalline. We think that upon crystallization a defective polycrystalline aggregate is formed. Upon decreasing the pressure the crystals are annealed, as is suggested by the increasingly strong polarization colors with decreasing pressure. Our Raman experiments also suggest that the facetlike crystalline samples are defective. When the pressure on a crystalline sample is reduced to the melting pressure, a few single crystals can be grown by increasing the pressure when only some grains are still present in the melt. Sometimes these single crystals have a clear matchboxlike shape. The C–O stretch Raman band for these single crystals is more distinctly split than for the crystalline faceted samples, which is in agreement with the observations of Mammone *et al.*[22]

From our x-ray diffraction, optical (polarization) microscopy and Raman experiments, we may safely conclude that clear samples are amorphous and facetlike samples (see Fig. 1) are crystalline. This correspondence allows us to study the kinetics of the pressure-induced amorphous to crystalline transition in methanol.

B. Crystallization kinetics

As mentioned before, for some of the samples between 5.0 and 10.5 GPa crystallization was observed, but others remained amorphous and vitrified at higher pressures. We have collected 300 measurements from 18 samples at pressures above the equilibrium freezing pressure (3.5 GPa), in which the pressure was measured within one minute and the phase of the sample was determined (crystalline vs amorphous). We have determined the fraction f of samples that crystallized within 1 min, for intervals of 0.5 GPa. From this fraction the steady-state nucleation rate can be calculated, provided that the transient time τ for the time-dependent nucleation, which is related to the induction time,[37] is much

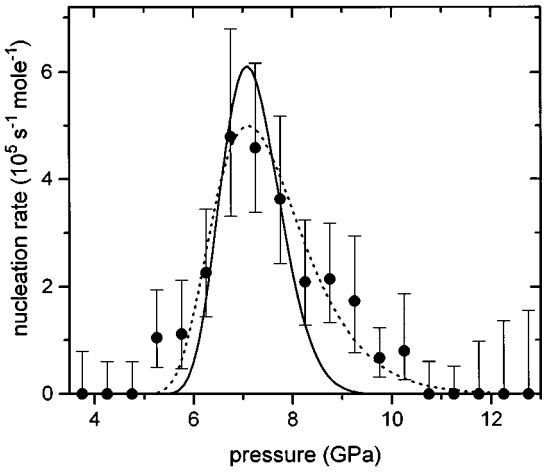

FIG. 3. Nucleation rate of methanol (in intervals of 0.5 GPa) as a function of pressure. The nucleation rate is calculated from the fraction of crystallization events f that take place within one minute upon reaching a certain pressure, using Eq. (1) and assuming an average value of $n=2\times10^{-8}$ mol for all the samples. In this figure 300 pressure measurements of 18 different samples above the melting pressure (3.5 GPa) have been collected. The error bars denote 68% of the binomial distribution for the crystallization fraction, for which the number of events and the number of trials are given by the experiments in that pressure interval. The solid line is a fit to the Turnbull–Fisher relation using the Stokes–Einstein relation to calculate the diffusion from the viscosity [Eq. (5)]. The dashed line is a fit to the Turnbull–Fisher equation with the diffusion taken from the crystal growth velocity data (Fig. 4).

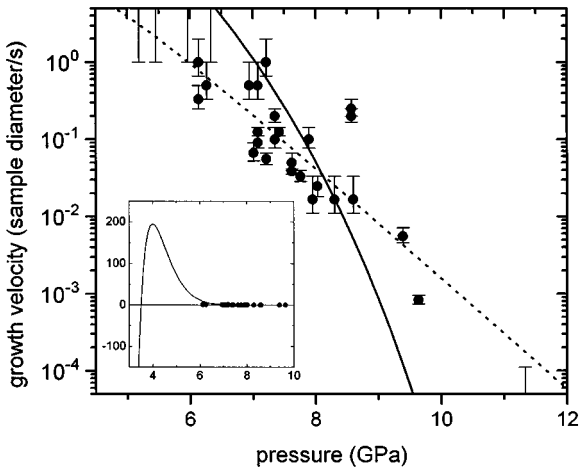

FIG. 4. Crystal growth velocity, which is the inverse of the time for the crystalline needles to grow from one point at the side of an $\simeq$0.1 mm diameter sample through the whole sample, as a function of pressure. The upper limit for the growth rate at 11.4 GPa is measured by pressurizing a growing crystalline structure at lower pressure. The solid line is a fit to the Wilson–Frenkel relation using the Stokes–Einstein relation to calculate the diffusion coefficient from the viscosity [Eq. (6)]. In the inset this line and the data are shown on a linear scale. Note that u is zero at the freezing pressure of 3.5 GPa. The transition region, where there is a finite nucleation rate, is in the tail of the growth velocity curve where diffusion completely determines the growth speed. The dashed line is the Wilson–Frenkel prediction, with a diffusion of the form given by Eq. (10) is fitted to the data, yielding a value of $v_{\rm hs}=7.0$ Å^3.

smaller than our observation time of $t=60$ s. We have verified that this is true at least in the pressure region that is of interest for the nucleation rate data,[38] between 5.0 and 10.5 GPa, and consequently we can calculate the steady-state nucleation rate per mole r from the crystallized fraction f

$$r=\frac{-\ln(1-f)}{nt}, \tag{1}$$

where the waiting time $t=60$ s and n is the number of moles in the sample, for which an estimated average value of $n=2\times10^{-8}$ mol has been used. In Fig. 3 the nucleation rate is plotted as a function of pressure, as determined from the crystallization fraction using Eq. (1). The liquid is superpressed up to about 5.0 GPa, which is inferred from the absence of nucleation. Above 5.0 GPa the nucleation rate increases, indicating that the difference in chemical potential between the crystalline state and the liquid is high enough to overcome the barrier for nucleation[39,40] and increases with pressure. We find a maximum in the nucleation rate at about 7.0 GPa and with further increasing pressure the crystallization rate goes down. Above 10.5 GPa the nucleation rate is negligible and in fact at these pressures we have never observed crystallization in any sample, even over periods of several days.

Because in the transition region the time it takes for the crystalline structure to grow through the whole sample is of the order of seconds to minutes, we have been able to measure the crystal growth velocity directly with optical microscopy [see also Fig. 1(b)].[41] In Fig. 4 the crystal growth velocity (the inverse of the time it takes for growing crystalline needles to occupy the whole sample of 0.1–0.2 mm diameter) is depicted as a function of pressure. It is clearly seen that for the whole transition region the growth velocity decreases with increasing pressure. The upper limit of the growth velocity at 11.3 GPa was obtained by increasing the pressure on a sample just after the crystalline structure had started to grow: After 900 s still no further growth of the crystals was observed. This clearly supports the notion obtained from Fig. 3 that at pressures above 10.5 GPa diffusion does not take place on experimental time scales.

The nucleation rate and the crystal growth velocity can be compared to classical nucleation theory. Following Kelton,[37] the nucleation rate per mole from the Turnbull–Fisher theory[42] can be written as

$$r=8\left(\frac{6}{\pi}\right)^{1/3}\frac{DN_A}{\lambda^2}\left(\frac{\gamma}{k_BT}\right)^{1/2}v^{1/3}\times\exp\left(-\frac{16\pi\gamma^3v^2}{3k_BT(\Delta\mu)^2}g(\theta)\right), \tag{2}$$

where D is the self diffusion coefficient, N_A is Avogadro's number, λ is the molecular jump distance (which is the mean free path for diffusion), γ is the surface free energy per unit area, v is the volume per molecule, and $\Delta\mu$ is the chemical potential difference between the initial phase and the nucleated phase. For heterogeneous nucleation, which we are likely to have because we find the nucleation centers usually at the edge of the sample, $g(\theta)$ accounts for the decrease of the nucleation barrier (θ is the wetting angle).[37] Based on the form for the solidification velocity as a function of temperature proposed by Wilson[43] and Frenkel,[44] the crystal growth velocity can be written as[45]

TABLE II. Parameters for classical nucleation theory and fitting parameters.

	A priori expected	Data fitted with free volume viscosity[a] and Stokes–Einstein	Data fitted with activated diffusion [Eq. (10)]
v_0 (Å^3)	67.6		
a_0 (Å)	1.91[a]		
γ (J m^{-2})	0.031		
η_0 (10^{-4} kg m^{-1} s^{-1})	5.5[a]		
D_0 (10^{-9} m^2 s^{-1})	2.3[b]		
A (m^3 mol^{-1})	2.2×10^{-6}	1.6×10^{-24}	1.5×10^{-26}
B (10^{17} J^2 m^{-6})	1.2 $g(\theta)$	1.3	0.80
C (10^{-38} m^4)	0.82 ϕ	17	0.85
$v_{\rm hs}$ (Å^3)	29		7.0

[a]From Ref. 21.
[b]From Ref. 48.

$$u=\frac{Dd\phi}{\lambda^2}\left[1-\exp\left(-\frac{\Delta\mu}{k_BT}\right)\right], \tag{3}$$

where d is the intermolecular spacing in the crystal along the growth direction and λ is again the mean free path for diffusion in the liquid. The term ϕ is the fraction of sites active in the crystallization process times $\exp(-\Delta S/k_B)$,[45] where ΔS is the entropy of fusion. The value of ϕ is of the order unity (somewhat smaller than one) but is not accurately known. To compare Eqs. (2) and (3) with the data in Figs. 3 and 4, we have to know the values and the pressure dependencies of the quantities involved. The *volume per molecule* for liquid methanol as a function of pressure, $v(p)$, is taken from Brown *et al.*[19] The *chemical potential difference*, $\Delta\mu(p)$ is obtained from integration of the equation of state of the liquid[19] and crystalline[35] phases. At the freezing point $\Delta\mu$ is zero and the density of crystalline methanol is assumed to be 5% higher than that of the liquid (this yields, e.g., $\Delta\mu=1.4\ k_BT$ at 8.0 GPa). The *surface free energy* is taken as half of the latent heat,[46] which is estimated from the slope of the melting line as determined by Sun *et al.*[47] and the estimated volume difference upon freezing (values of the constants used are given in Table II). The *mean free path* in the liquid λ scales with the volume per molecule: $\lambda(p)=v(p)/\pi a_0^2$, where a_0 is the hard-sphere radius a_0.[21] The *intermolecular spacing of the crystal planes d* is calculated from the volume per molecule in the crystalline phase $d(p)=[3v_c(p)/4\pi]^{1/3}$. The *self-diffusion* can be obtained from the viscosity. For simple liquids but also for materials where crystallization involves molecular reorientation or breaking of directional bonds at the interface, the diffusion is known to be inversely proportional to the viscosity.[39] Using the free volume model for the viscosity η that was obtained from the viscosity data as a function of pressure by Cook *et al.*,[21] the self-diffusion coefficient can be calculated using the Stokes–Einstein relation

$$D=\frac{k_BT}{6\pi a_0\eta}, \tag{4}$$

where a_0 is again the hard-sphere radius (see Table II).

Collecting the pressure independent quantities in newly defined constants, we can rewrite Eqs. (2) and (3)

$$r(p)=A\,\frac{D(p)}{[v(p)]^{5/3}}\exp\left[-B\left(\frac{v(p)}{\Delta\mu(p)}\right)^2\right], \tag{5}$$

$$u(p)=C\,\frac{D(p)[v_c(p)]^{1/3}}{[v(p)]^2}\left[1-\exp\left(-\frac{\Delta\mu(p)}{k_BT}\right)\right], \tag{6}$$

with

$$A=\frac{8}{\pi^2}\left(\frac{6}{\pi}\right)^{1/3}N_Aa_0^4\left(\frac{\gamma}{k_BT}\right)^{1/2}, \tag{7}$$

$$B=\frac{16\pi\gamma^3}{3k_BT}\,g(\theta), \tag{8}$$

$$C=\left(\frac{3\pi^5}{4}\right)^{1/3}a_0^4\phi. \tag{9}$$

We can now fit the Eqs. (5) and (6) to the data in Figs. 3 and 4, respectively, using the diffusion coefficient $D(p)$ obtained from the free volume model for the viscosity in combination with Eq. (4) and using A, B, and C as adjustable parameters. The fits are represented by the solid lines in Figs. 3 and 4, and the corresponding values for the adjustable parameters are given in Table II. We can compare these parameters with the values obtained from the prediction of classical nucleation theory in combination with the Stokes–Einstein equation (Table II). The parameters B and C are in surprisingly good agreement with the expected values. However, the prefactor A in the expression for the nucleation rate is 18 orders of magnitude *lower* than the anticipated value (the implications of the values for the adjustable parameters are discussed below). Nevertheless, the trends in both the nucleation rate and the growth velocity data are satisfactorily described by the classical nucleation theory. The fit to the nucleation rate (Fig. 3) clearly shows that beyond a certain pressure the difference in chemical potential between liquid and crystalline phases is large enough to overcome the barrier for nucleation and the nucleation rate increases with pressure. At about 7 GPa, however, the decreasing diffusion starts to suppress the nucleation rate and finally nucleation centers cannot be formed at the highest pressures. The fit to the crystal growth velocity shows that in the transition region the growth velocity is completely determined by the diffusion. In fact, this is the reason why the growth velocity is low enough in the transition region to be observed visually.

One of the central assumptions made in our description of the data above is to use the Stokes–Einstein equation [Eq. (4)] to calculate the diffusion from known viscosity data.[21] We have verified that scaling the hard-sphere radius with the volume per molecule yields nearly the same fits. Another way to analyze the data is by fitting a pressure dependence of the self-diffusion coefficient to the crystal growth velocity, because in the transition region this velocity depends very weakly on $\Delta\mu$.[49] In a simple conception of diffusion of hard spheres, the work that has to be done for a particle to diffuse by a nearest neighbor distance is $pv_{\rm hs}$, where $v_{\rm hs}$ is the hard-sphere volume. The diffusion coefficient can then be written as

$$D(p)=D_0\,\exp\left(-\frac{pv_{\rm hs}}{k_BT}\right), \tag{10}$$

where D_0 is the diffusion constant at ambient pressure (see Table II). Combining Eqs. (3) and (10), we can fit our crystal growth data between 6 and 10 GPa, using v_{hs} as an adjustable parameter in addition to C. The result is shown in Fig. 4 as the dotted line and the agreement with the growth velocity data has clearly been improved. The fit yields a value of 7.0 Å^3 for v_{hs} and, as can be seen in Table II, this value compares satisfactorily with the value calculated from the hard-sphere radius $(4/3)\pi a_0^3 = 29$ Å^3. Also the value of C is in close agreement with the expected value. With this experimentally determined diffusion the nucleation rate data of Fig. 3 can be fitted again using Eq. (5). The result is shown in Fig. 3 as the dotted line and also for the nucleation rate the agreement has clearly been improved with this new form for the diffusion coefficient. The good agreement for the parameter B in the exponent of the nucleation rate indicates that our estimate for the free energy barrier for nucleus formation is correct and that the barrier lowering factor $g(\theta)$ is of the order 1. Thus we can safely estimate the critical cluster size n^* [37] as a function of pressure, and at the onset of crystallization (5.0 GPa) we obtain $n^* \sim 10^2$. The parameter A for the nucleation rate is again much lower than the expected value. In many cases, classical nucleation theory predicts a nucleation prefactor A different from the experimental data by many orders of magnitude. In temperature dependent studies the predicted value of A is often too low, which is attributed to a negative entropy contribution due to ordering of the liquid near the interface (see Kelton[37] and Oxtoby[50]). In contrast, in this pressure dependent study the predicted value of A is much too high for which we have no explanation. The parameter C for the growth velocity, however, agrees very well with the anticipated value. This is somewhat puzzling, because both prefactors scale with the same diffusion constant. Although our findings comply with the statements that the prefactor A in the nucleation rate is difficult to estimate, both the position of the maximum (determined by the parameter B) as well as the pressure dependence of the nucleation rate are in excellent agreement with the predictions from classical nucleation theory, if the activated diffusion is used that is obtained from the growth velocity.[51] Furthermore, the excellent description of our growth velocity data with Eqs. (3) and (10) shows that the crystal growth velocity in methanol at high pressure is diffusion limited and not collision limited.[52]

So far we have shown that the activated diffusion obtained from the crystal growth velocity data [Eq. (10) with $v_{hs} = 7.0$ Å^3], indeed applies to methanol in the transition region. To see how this activated diffusion compares to a diffusion obtained from a free volume model (the inverse of the free volume viscosity taken from Ref. 21), $\ln(D/D_0)$ is plotted as a function of pressure in Fig. 5 for both cases. The points are the normalized inverse viscosity data of Cook *et al.*,[21] the solid line is their free volume model fitted to the experimental data,[21] and the dotted line is the pressure dependence of the activated diffusion that describes both our nucleation rate data and our crystal growth velocity data. Up to about 6 GPa the fitted activated diffusion is indeed found to be exactly inversely proportional to the viscosity, but at higher pressures the viscosity increases much more with

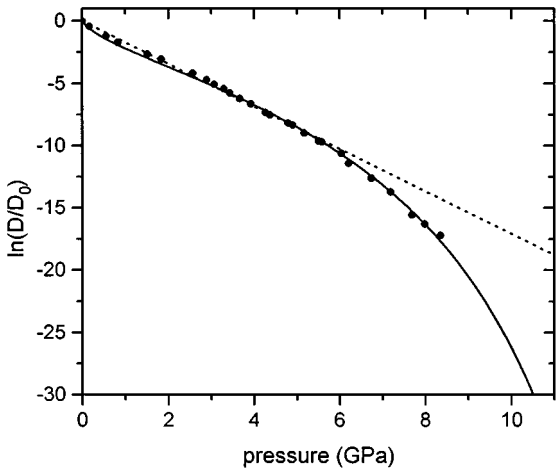

FIG. 5. Logarithm of the normalized self-diffusion coefficient as a function of pressure. The dashed line is the activated diffusion coefficient, Eq. (10) with $v_{hs} = 7.0$ Å^3, obtained from a fit to the growth velocity data, which also describes the nucleation rate data. The dots are the inverse normalized experimental viscosity data as obtained by Cook *et al.* (Ref. 21). The solid line is the diffusion calculated from the free volume model fitted to viscosity data (Ref. 21), assuming an inversely proportionality between diffusion and viscosity [from this model a glass transition pressure of 11 ± 0.7 GPa was obtained (Ref. 21)]. It is seen that up to about 6 GPa the diffusion is indeed inversely proportional to the viscosity, but that above this pressure the diffusion decreases more slowly than that the viscosity increases.

pressure than the diffusion decreases. It is not clear to us why this deviation occurs above 6 GPa. Maybe the hydrogen bonded methanol chains start to form a rigid network that has a large viscosity as a whole, but in which self-diffusion of molecules can still occur by collective processes. Our observation of an activated diffusion coefficient which deviates from the Stokes–Einstein prediction above a pressure that is smaller than the glass transition pressure is reminiscent of findings in low-temperature liquids: Upon cooling a liquid, at a temperature above the glass transition temperature a cross over is observed from a Stokes–Einstein diffusion to an activated hopping process.[53,54]

Our results of the crystallization kinetics are somewhat in contrast to the expectation of Angell,[6] who states that at high pressures ''all liquids should begin to resemble the hard-sphere fluid'' and that it is not clear whether the glassy state survives ''because of the decreasing gap in configuration space between the liquid and the crystal, and the consequent increase in crystallization kinetics.'' First of all, we do not think that any strongly compressed substance behaves as a hard-sphere system.[55,56] It might be appealing to replace the steep repulsive potential of compressed systems with a hard wall potential. However, the essential difference is that infinitely hard systems are purely entropic whereas real systems develop a large internal energy that competes with entropy in the free energy. Second, we found that beyond the transition region, methanol stays in the glassy state at least up to 33 GPa. In the description of the glass with a potential energy hypersurface Φ, the relaxation kinetics are determined not only by the distance between the energy barriers in Φ, but also by the height of the barriers. Under compression the barrier distance is reduced, but simultaneously the barrier height is increased, and both dimensions are deter-

mined by the detailed microscopic interactions. Hence, it is not intuitively clear whether relaxation is slower or faster in compressed glasses compared to temperature quenched glasses. This is illustrated by the following example. Methanol seems to be arrested in the glassy state more easily by compression than upon cooling: The cooling rate to obtain methanol glass is so high that in practice only vapor deposition is used to obtain this phase. Ethanol in contrast, which is relatively easily frozen into a glass at 97 K for cooling rates >0.5 K/s,[57] is found to always crystallize under pressure at 1.78 GPa.[22]

IV. CONCLUSIONS

We have performed x-ray diffraction, optical (polarization) microscopy, Raman spectroscopy, and hydrostaticity measurements to study methanol at pressures up to 33 GPa. At high pressures methanol can be solidified either in a crystalline or in a glassy phase. The crystalline phase, which we have identified with several of the experimental techniques used, is easily recognized with optical microscopy, because it has a facetlike morphology. In analogy with solid methanol at low temperature, there is a transition region where crystallization takes place. When this transition region, that ranges from 5.0 to 10.5 GPa, is surpassed quickly enough (within a few seconds) a glass is formed. The recognition of a transition region with a pressure dependent probability for crystallization resolves recent doubts of Cook *et al.*[21] about previous studies of Piermarini *et al.*[20]

Between the freezing pressure of 3.5 GPa and 5.0 ± 0.5 GPa crystallization is never observed and in this region methanol is a superpressed liquid. Above 5.0 ± 0.5 GPa there is a finite nucleation rate that increases with pressure due to the increasing difference of the chemical potential of the liquid and crystalline phases. For pressures higher than 7.0 ± 0.5 GPa the nucleation rate decreases. This is caused by the decrease in diffusion with increasing pressure, which is supported by the observation that the crystal growth rate decreases with pressure in this region. Above 10.5 ± 0.5 GPa, diffusion is so small that nucleation centers cannot be formed on experimental time scales and the methanol has been compressed into a glass.

The onset of the glassy phase for methanol as obtained from Fig. 3, 10.5 ± 0.5 GPa, is in excellent agreement with the anticipated pressure of 11.0 ± 0.7 GPa, obtained from an extrapolation of the viscosity to a value of 10^{13} P.[21] It coincides also notably well with the glass transition pressure of 10.8 GPa for the mixture 4:1-M:E,[23] in which the ethanol suppresses crystallization.

The pressure dependence of both the nucleation rate and the crystal growth velocity are in qualitative agreement with Turnbull–Fisher and Wilson–Frenkel-type expressions, using the Stokes–Einstein equation to calculate the diffusion from the viscosity. The pressure dependent nucleation rate data are in accurate agreement with classical nucleation theory if an activated diffusion is used, that is obtained from the crystal growth velocity data. This strongly indicates that both kinetic processes are limited by the same self-diffusion process.

The activated diffusion coefficient, which describes both our growth velocity and our nucleation rate data, is found to deviate above 6 GPa from the diffusion coefficient expected from a free volume model for the viscosity. Detailed information about the self-diffusion is necessary to understand relaxation processes in glasses, because relaxation is directly related to individual movement of the particles. Because the detailed microscopic interactions that determine the relaxation kinetics behave differently as a function of pressure than as a function of temperature, pressure dependent studies of the glass transition can provide new information about the microscopic dynamics.

ACKNOWLEDGMENTS

We thank Richard Nelmes, Malcolm McMahon, Dave Allen, Nick Wright, and Hengda Liu for great help with the x-ray diffraction experiments and the use of their equipment. Graham Bushnell-Wye is acknowledged for help with the operation of the x-ray beam line at SRS Daresbury. Both Dave Mao and Daniel Hausermann kindly loaned a DAC. Jan Schouten and Willem Koster are thanked for the use of their Raman setup. We appreciate the continuous encouragement of Ad Lagendijk and fruitful discussions with Daan Frenkel and Wim van Saarloos. The SRS Daresbury Laboratory is acknowledged for hospitality and financial support. The work of M.J.P.B. is part of the research program of the Stichting Fundamenteel Onderzoek van de Materie (Foundation for Fundamental Research on Matter) and was made possible by financial support from the Nederlandse Organisatie voor Wetenschappelijk Onderzoek (Netherlands Organization for the Advancement of Science).

[1] *Glass: Science and Technology*, edited by D. R. Uhlmann and N. J. Kreidl (Academic, New York, 1983), Vol. I.
[2] W. Götze, in *Liquids, Freezing, and Glass Transition*, edited by J. P. Hansen, D. Levesque, and J. Zinn-Justin (North-Holland, Amsterdam, 1991), Les Houches, Session LI, p. 289.
[3] G. Adam and J. H. Gibbs, J. Chem. Phys. **43**, 139 (1965).
[4] U. Mohanty, Phys. Rev. A **34**, 4993 (1986).
[5] F. H. Stillinger, Phys. Rev. B **34**, 2409 (1990).
[6] C. A. Angell, J. Non-Cryst. Solids **13**, 131 (1991).
[7] U. Mohanty, I. Oppenheim, and C. H. Taubes, Science **266**, 425 (1994).
[8] W. F. Oliver, C. A. Herbst, S. M. Lindsay, and G. H. Wolf, Phys. Rev. Lett. **67**, 2795 (1991).
[9] C. A. Herbst, R. L. Cook, and H. E. King, Nature (London) **361**, 518 (1993).
[10] C. Alba-Simionesco, J. Chem. Phys. **100**, 2250 (1994).
[11] D. C. Steytler, J. C. Dore, and D. C. Montague, J. Non-Cryst. Solids **74**, 303 (1985).
[12] M. Haughney, M. Ferrario, and I. R. McDonald, J. Phys. Chem. **91**, 4934 (1987).
[13] P. Sindzingre and M. L. Klein, J. Chem. Phys. **96**, 4681 (1992).
[14] M. Falk and E. Whalley, J. Chem. Phys. **34**, 1554 (1961).
[15] A. B. Dempster and G. Zerbi, J. Chem. Phys. **54**, 3600 (1971).
[16] M. Sugisaki, H. Suga, and S. Seki, Bull. Chem. Soc. Jpn. **41**, 2586 (1968).
[17] F. J. Berjemo, J. Alonso, A. Criado, F. J. Mompeán, J. L. Martínez, M. Carcía-Hernández, and A. Chahid, Phys. Rev. B **46**, 6173 (1992).
[18] K. J. Tauer and W. N. Lipscomb, Acta Cryst. **5**, 606 (1952).
[19] J. M. Brown, L. J. Slutsky, K. A. Nelson, and L.-T. Cheng, Science **241**, 65 (1988).
[20] G. J. Piermarini, S. Block, and J. D. Barnett, J. Appl. Phys. **44**, 5377 (1973).
[21] R. L. Cook, C. A. Herbst, and H. E. King, J. Phys. Chem. **97**, 2355 (1993).
[22] J. F. Mammone, S. K. Sharma, and M. Nicol, J. Phys. Chem. **84**, 3130 (1980).

[23] J. H. Eggert, L. Xu, R. Che, and L. Chen, J. Appl. Phys. **72**, 2453 (1992).
[24] A. R. Ubbelohde, *The Molten State of Matter* (Wiley, Chichester, 1978), Chap. 16.
[25] W. R. Russel, Phase Transitions **21**, 127 (1990), and references therein.
[26] J. K. G. Dhont, C. Smits, and H. N. W. Lekkerkerker, J. Colloid Interface Sci. **152**, 386 (1991).
[27] K. Schätzel and B. J. Ackerson, Phys. Rev. Lett. **68**, 337 (1992); Phys. Rev. E **48**, 3766 (1993).
[28] A. Jayaraman, Rev. Sci. Instrum. **56**, 1013 (1986).
[29] J. D. Barnett, S. Block, and G. J. Piermarini, Rev. Sci. Instrum. **44**, 1 (1973).
[30] This is more reliable than monitoring the linewidth of the Ruby fluorescence; see, e.g., Ref. 20 for argumentation as well as application of both techniques.
[31] G. Bushnell-Wye and R. J. Cernik, Rev. Sci. Instrum. **63**, 999 (1992).
[32] R. J. Nelmes and M. I. McMahon, J. Synchr. Rad. **1**, 69 (1994), and references therein.
[33] R. O. Piltz, M. I. McMahon, J. Crain, P. D. Hatton, R. J. Nelmes, R. J. Cernik, and G. Bushnell-Wye, Rev. Sci. Instrum. **63**, 700 (1992).
[34] K. M. Yenice, S. A. Lee, and D. W. Downs, Mol. Phys. **69**, 973 (1990).
[35] W. L. Vos and M. J. P. Brugmans (unpublished).
[36] B. E. Warren, *X-ray Diffraction* (Dover, New York, 1969), p. 30.
[37] K. F. Kelton, in *Solid State Physics: Advances in Research and Applications*, edited by H. Ehrenreich and D. Turnbull (Academic, Boston, 1991), Vol. 45, p. 75.
[38] Using Eq. (6.3) of Ref. 37 and the parameters given in Table II and discussed in Sec. III B, we estimate the transient time τ to range from 0.7 μs at 5.0 GPa to 7 ms at 10.5 GPa, which is indeed much smaller than our waiting time of 60 s.
[39] D. R. Uhlmann and H. Yinnon, in Ref. 1, Chap. 1.
[40] W. Kurz and D. J. Fisher, *Fundamentals of Solidification*, 3rd ed. (Trans. Tech., Switzerland, 1989).
[41] Out of plane velocity components have been neglected because the samples are much wider than thick.
[42] D. Turnbull and J. C. Fisher, J. Chem. Phys. **17**, 71 (1949).
[43] H. A. Wilson, Proc. Cambridge Philos. Soc. **10**, 25 (1898); Philos. Mag. **50**, 238 (1900).
[44] J. Frenkel, Phys. Z. Sowjetunion **1**, 498 (1932).
[45] K. A. Jackson, in *Crystal Growth and Characterization*, edited by R. Ueda and J. B. Mullin (North-Holland, Amsterdam, 1975), p. 21.
[46] K. A. Jackson and B. Chalmers, Can. J. Phys. **34**, 473 (1956).
[47] T. F. Sun, J. A. Schouten, N. J. Trappeniers, and S. N. Biswas, Ber. Bunsenges. Phys. Chem. **92**, 652 (1988).
[48] Landolt–Börnstein II, *Eigenschaften der Materie in ihren Aggregatzuständen* (Springer, Berlin, 1969), 6th ed., Vol. 5a, p. 591.
[49] It is not possible to obtain better fits to both the nucleation rate and the crystal growth rate for several other forms of $\Delta\mu$, using the diffusion taken from the viscosity of Cook *et al.* (Ref. 21) in combination with the Stokes–Einstein equation.
[50] D. W. Oxtoby, J. Phys.: Condens. Matter **4**, 7627 (1992).
[51] This suggests that the pre-exponential factor for the nucleation rate should indeed contain the diffusion coefficient [see Eq. (2)], which was recently doubted by Oxtoby (Ref. 50).
[52] J. Q. Broughton, G. H. Gilmer, and K. A. Jackson, Phys. Rev. Lett. **49**, 1496 (1982).
[53] E. Rössler, Phys. Rev. Lett. **65**, 1595 (1990).
[54] J.-L. Barrat and M. L. Klein, Ann. Rev. Phys. Chem. **42**, 23 (1991).
[55] J. Schouten, Fluid Phase Eq. **76**, 151 (1992).
[56] W. L. Vos and J. A. Schouten, Low Temp. Phys. **19**, 338 (1993).
[57] O. Haida, H. Suga, and S. Seki, J. Chem. Thermodynamics **9**, 1133 (1977).